THE PUBLISHING HOUSE
OF THE ROMANIAN ACADEMY

PROCEEDINGS OF THE ROMANIAN ACADEMY, Series A,
Volume 24, Number 1/2023, pp. 27–34
DOI: 10.59277/PRA-SER.A.24.1.04

STUDY OF SOLAR CELLS STRUCTURES BASED ON PEROVSKITE AND NANOPARTICLES

Mahassen H. ELBLBEISI [1], Mohammed M. SHABAT [2]

[1] Islamic University of Gaza, Physics Department, P.O.Box 108, Gaza Strip, Palestine
[2] Northumbria University, Department of Mathematics, Physics and Electrical Engineering, Newcastle upon Tyne, NE1 8ST, United Kingdom
Corresponding author: MAHASSEN H Elblbeisi, Palestine, E-mail: mahassenhasan@gmail.com

Abstract. Researchers and scientists working in the field of energy conversion have become interested in the rapidly developing new class of solar cells based on mixed organic-inorganic halide perovskite semiconductors over the past few years. Here we study the transmission of assumed solar cell structures based on nanoparticles and $CH_3NH_3PbI_3$, $CH_3NH_3PbBr_3$, and $CH_3NH_3PbI_2Br$ perovskite types by using the transfer matrix method (TMM). We found that as the nanoparticle volume fraction increases, the transmission decreases. Cells doped with aluminum nanoparticles showed the best transmission values. And transmission values in all wavelength ranges are better than those in the range of approximately 300–500.

***Key words**:* solar cells, perovskite, transfer matrix method, transmission, nanoparticles, ARC.

1. INTRODUCTION

Due to the lack of conventional energy resources and environmental concerns, solar photovoltaic technology has received a remarkable and growing amount of attention in recent decades [1, 2]. A clean energy source with high availability and straightforward application potential is solar energy. However, for solar cells to be more competitive with known energy sources, they must be more efficient [1]. This necessitates the development of new solar cell designs based on the concepts of waveguides and novel antireflection coatings structures [2–5]. Due to their uncomplicated design and technological application, antireflection coatings for the visible and infrared regions have also long drawn significant research and development. However, nanoparticle technology has only lately been applied to improve thin film solar cells [1]. Adding nanoparticles to the cover region, for instance, can enhance antireflection coatings (ARC), resulting in a reduction in reflection and an increase in transmission [6, 7]. Also, Perovskite materials have extensively appeared in terms of their power conversion efficiencies(PCEs) since the emergence of organic-inorganic halide perovskite materials as effective light harvesters according to their excellent efficiency and low cost [8–10].

Based on previous research in this field [11, 12], research aimed to develop and study a multilayer waveguide solar cell with three different perovskite types and nanoparticles.

The type of nanoparticle, its fraction, the thickness of the cover layer, and the type of perovskite are all taken into consideration while examining the impact of the suggested waveguide structure on the transmitted light.

2. THEORY

This work examines a novel structure based on perovskite and metal nanoparticles (NPs) doped in a glass. Gold (Au, $\varepsilon_i = -1.45$), Aluminium (Al, $\varepsilon_i = 4.7$), and Silver (Ag, $\varepsilon_i = -2.55$) NPs doped on the glass cover ($\varepsilon = 1.212$), another two layers of titanium dioxide ($d_1 = 90$ nm, $\varepsilon_1 = 1.549$), and perovskite types (($CH_3NH_3PbI_3$, $\varepsilon_2 = 10$), ($CH_3NH_3PbBr_3$, $\varepsilon_2 = 17$), and ($CH_3NH_3PbI_2Br$, $\varepsilon_2 = 15$)) with ($d_2 = 250$ nm) sandwiched between it and silicon substrate ($\varepsilon = 1.942$) [7, 13–14]. As seen in Fig. 1.

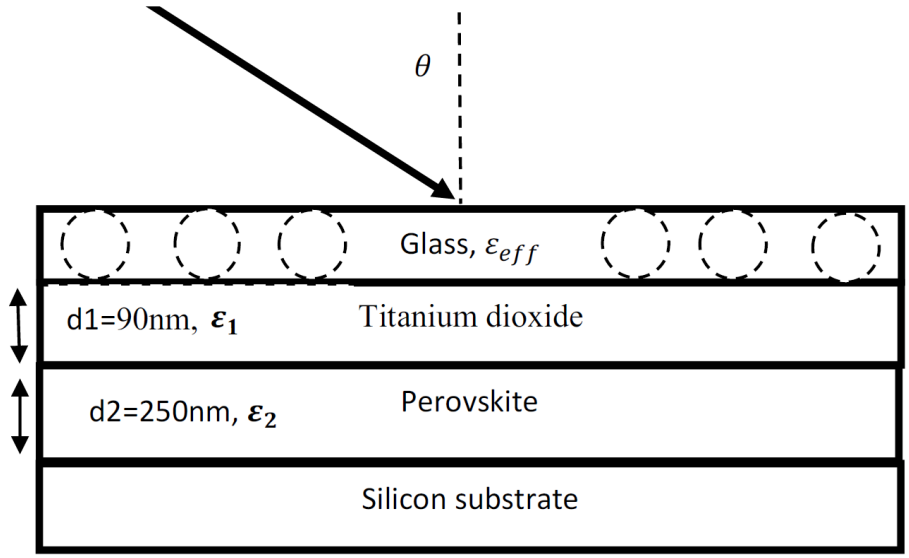

Fig. 1 – The design of the model structure.

The results of the average transmittance for the ARC have been obtained using the Maple 17 program. Here, we study stable and economical perovskite types, and we used nanoparticles to boost efficiency [15]. The effective permittivity of composite materials constructed by metal nanoparticles in the glass host is calculated using the Maxwell Garnett effective medium method. The effective permittivity is determined using the following formulas [12]:

$$\varepsilon_{eff} = \varepsilon_b \frac{\varepsilon_i (1+2f) + 2\varepsilon_b (1-f)}{\varepsilon_i (1-f) + \varepsilon_b (2+f)} \tag{1}$$

where: (ε_b) is the Permittivity of glass ε_i is the metal nanoparticle's permittivity, and f is the particle's volume fraction in the host medium.

We examine light strikes from the air on the cell at all incident angles (0–90) degrees to show the efficacy of the suggested configuration. To calculate the transmission (T), Maxwell's equations are utilized to construct a matrix formulation of the boundary conditions at the film surfaces. The following definition applies to the 2×2 transfer matrix, which connects the field components at two subsequent borders [16]:

$$M_l = \begin{bmatrix} \cos(\delta_l) & \left(\frac{i \sin(\delta_l)}{\gamma_l}\right) \\ i\gamma_l \sin(\delta_l) & \cos(\delta_l) \end{bmatrix} \tag{2}$$

$$\begin{bmatrix} E_a \\ B_a \end{bmatrix} = M_l \begin{bmatrix} E_b \\ B_b \end{bmatrix} \tag{3}$$

where: $\delta_l == \left(\frac{2\pi}{\lambda}\right) n_l d_l \cos(\theta_l)$ is the phase difference, d_l its thickness, θ_l is the propagation angle, and γ_l is the optical admittance.

$$\gamma_l = \begin{cases} n_l \cos(\theta_l), & \text{TE polarization} \\ n_l / \cos(\theta_l), & \text{TM polarization} \end{cases}. \tag{4}$$

The total transfer matrix (M_T) for (m) layers is defined as follows:

$$M_T = M_1 M_2 M_3 \ldots M_m = \prod_{l=1}^{m} M_l = \begin{bmatrix} m_{11} & m_{12} \\ m_{21} & m_{22} \end{bmatrix} \tag{5}$$

From the components in the system of the transfer matrix, the transmission coefficient and transmittance can be determined as follows:

$$t = \frac{\det M}{M_{22}}, \quad r = \frac{M_{21}}{M_{11}} \tag{6}$$

$$R = r^2 \cdot T = 1 - R\,. \tag{7}$$

The average transmittance (T) of a solar cell is stated as follows:

$$T = \frac{T_{TE} + T_{TM}}{2}\,. \tag{8}$$

3. RESULTS AND DISCUSSIONS

Here, we study the average transverse magnetic (TM) and transverse electric (TE) transmittance for the model and analyzed it and hence the results:

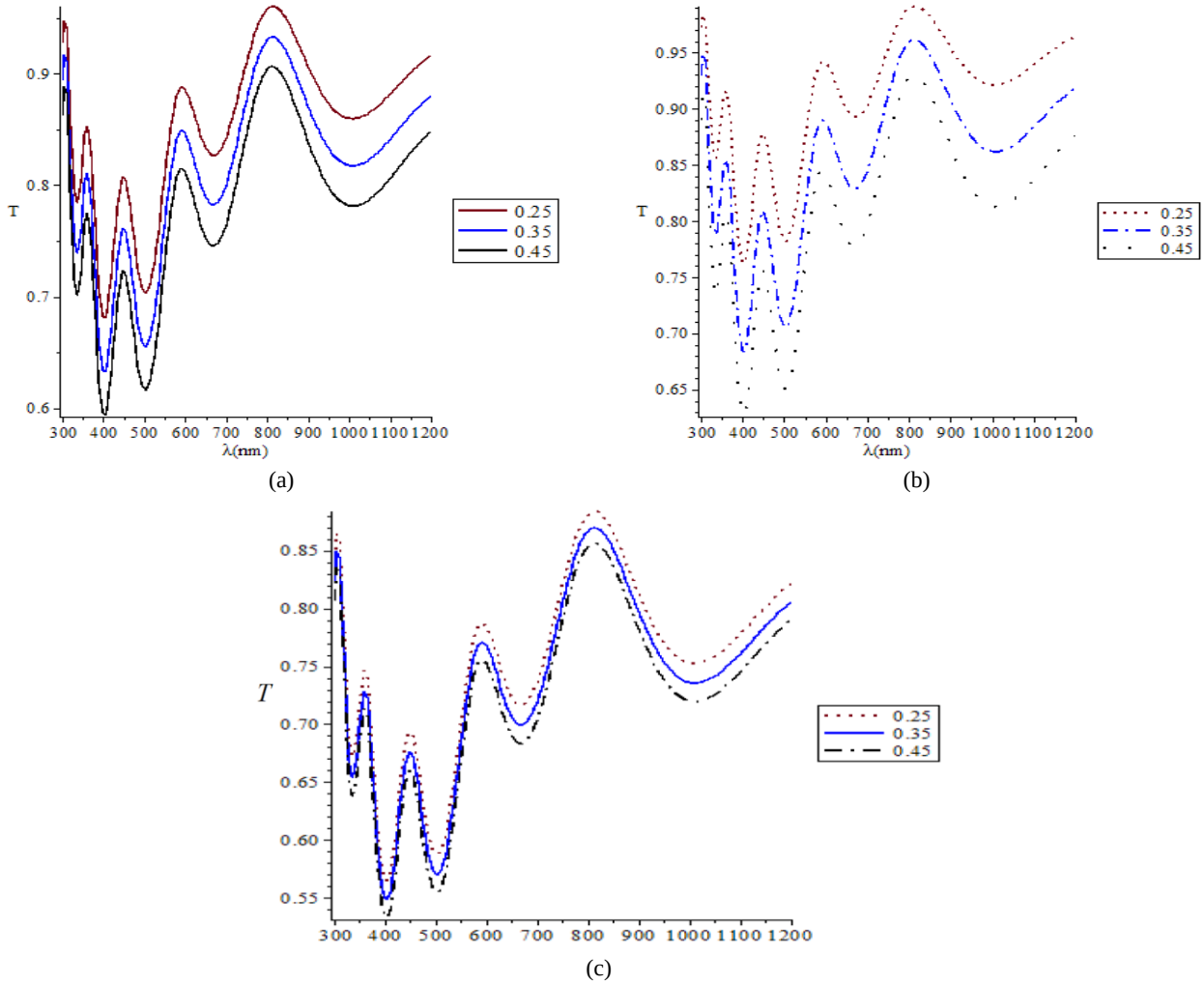

Fig. 2 – The transmitted light of the proposed structure for the different volume fractions of: a) Ag, b) Al, c) Au and wavelength, and $CH_3NH_3PbI_3$.

Figure 2 illustrates the transmittance of the proposed structure with $CH_3NH_3PbI_3$ Perovskite for different nanoparticles (Ag, Al, and Au) and different nanoparticles volume fractions (f = 0.05, 0.25, 0.35, and 0.45). In general, as the volume fraction increases the transmittance decreases in the same cell, but when we compare cells with each other we find that aluminum nanoparticles have a transmittance value better than silver and gold nanoparticles.

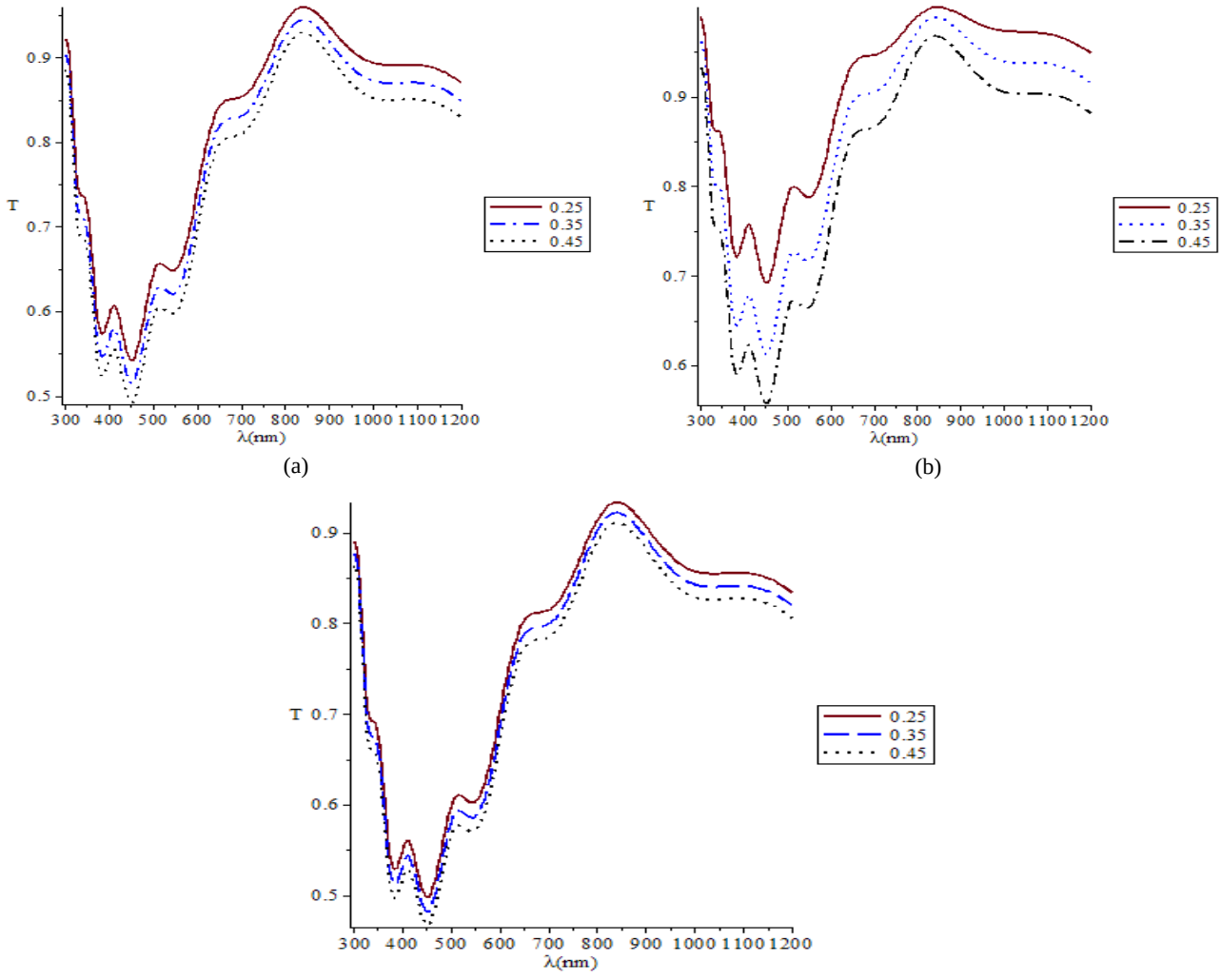

Fig. 3 – The transmitted light of the proposed structure for the different volume fractions of: a) Ag, b) Al, c) Au, and wavelength, and $CH_3NH_3PbBr_3$.

Figure 3 displays the transmitted light of the proposed structure for the different volume fractions (f = 0.25, 0.35, and 0.45) of (Ag, Al, Au) and wavelength, and $CH_3NH_3PbBr_3$, perovskites type.

The cell transmission minimum value is up to 55% of the incident light with aluminum, and 45% with silver and gold. The maximum value ups to approximately 95% in all cells.

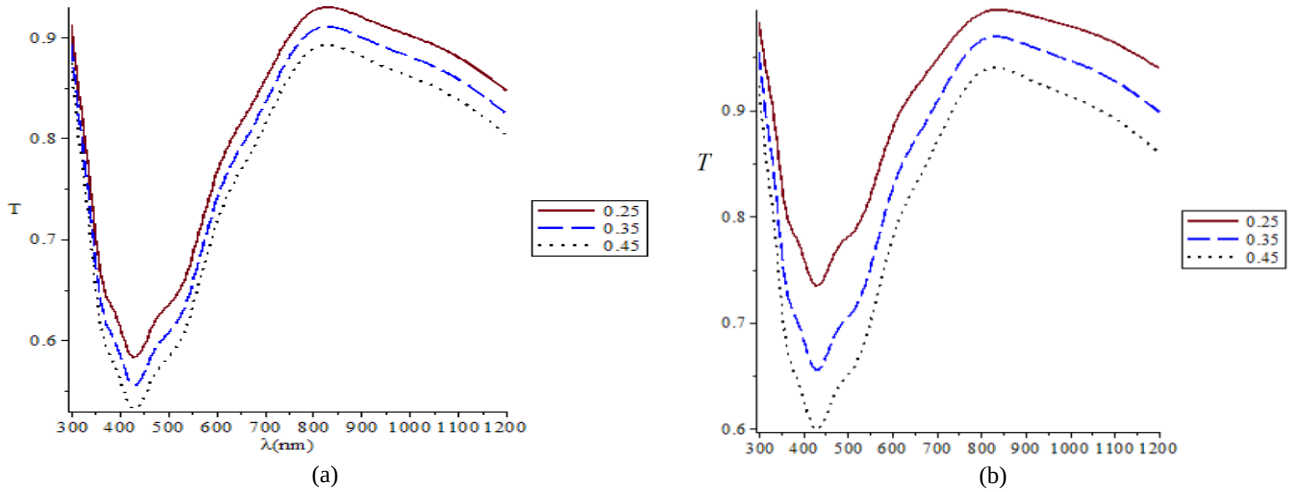

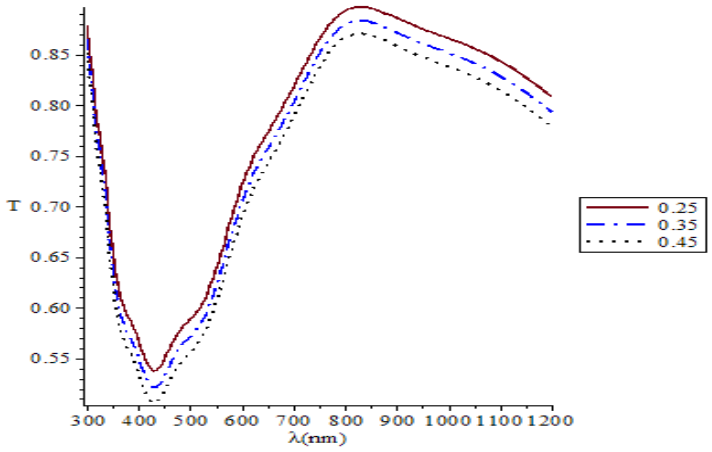

(c)

Fig. 4 – The transmitted light of the proposed structure for the different volume fractions of: a) Ag, b) Al, c) Au, and wavelength, and $CH_3NH_3PbI_2Br$.

Figure 4 shows the transmitted light of the proposed structure for the different volume fractions (f = 0.25, 0.35, and 0.45) of (Ag, Al, Au) and wavelength, and $CH_3NH_3PbI_2Br$ perovskites type. It shows that the difference in the volume fraction of silver and gold has a slight effect in comparison with the aluminum volume fraction difference.

Figures 3 and 4 find that the minimum value for the transmission goes to the high wavelength from approximately 400 – 425 – 450 nm when we transmit $CH_3NH_3PbI_3$ to $CH_3NH_3PbI_2Br$ to $CH_3NH_3PbBr_3$.

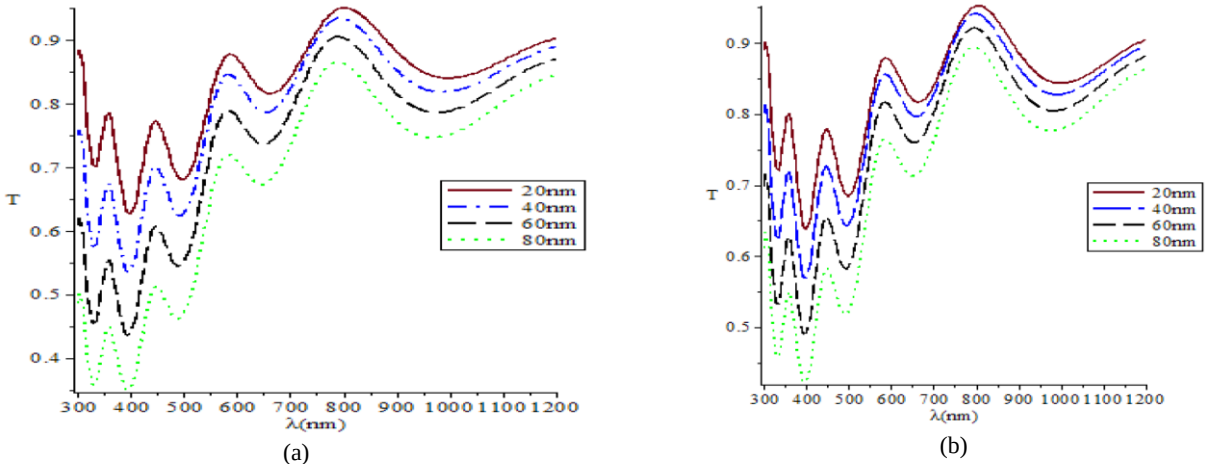

(a) (b)

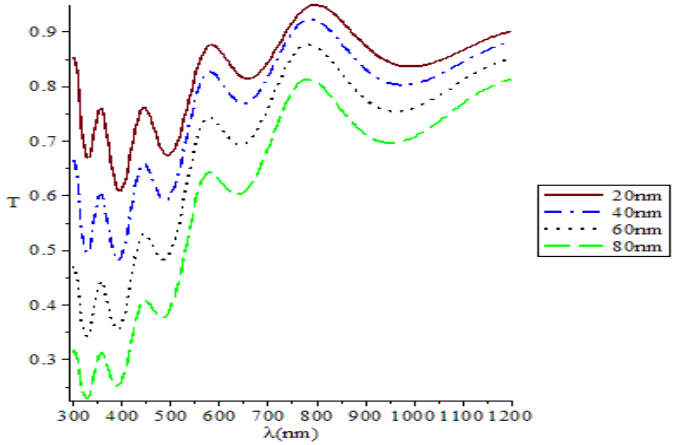

(c)

Fig. 5 – The transmitted light of the proposed structure for different active layer thicknesses doped by: a) Ag, b) Al, c) Au, and wavelength, and $CH_3NH_3PbI_3$.

Figure 5 plots the transmitted light of the proposed structure with $CH_3NH_3PbI_3$ perovskite type and glass layer doped by (Ag, Al, and Au) nanoparticles at $f = 0.25$ with different thicknesses 20, 40, 60, 80 nm and wavelength.

It shows that as active layer thickness increases the transmission decreases, and 20 nm transmissions have a very high value for each different parameter.

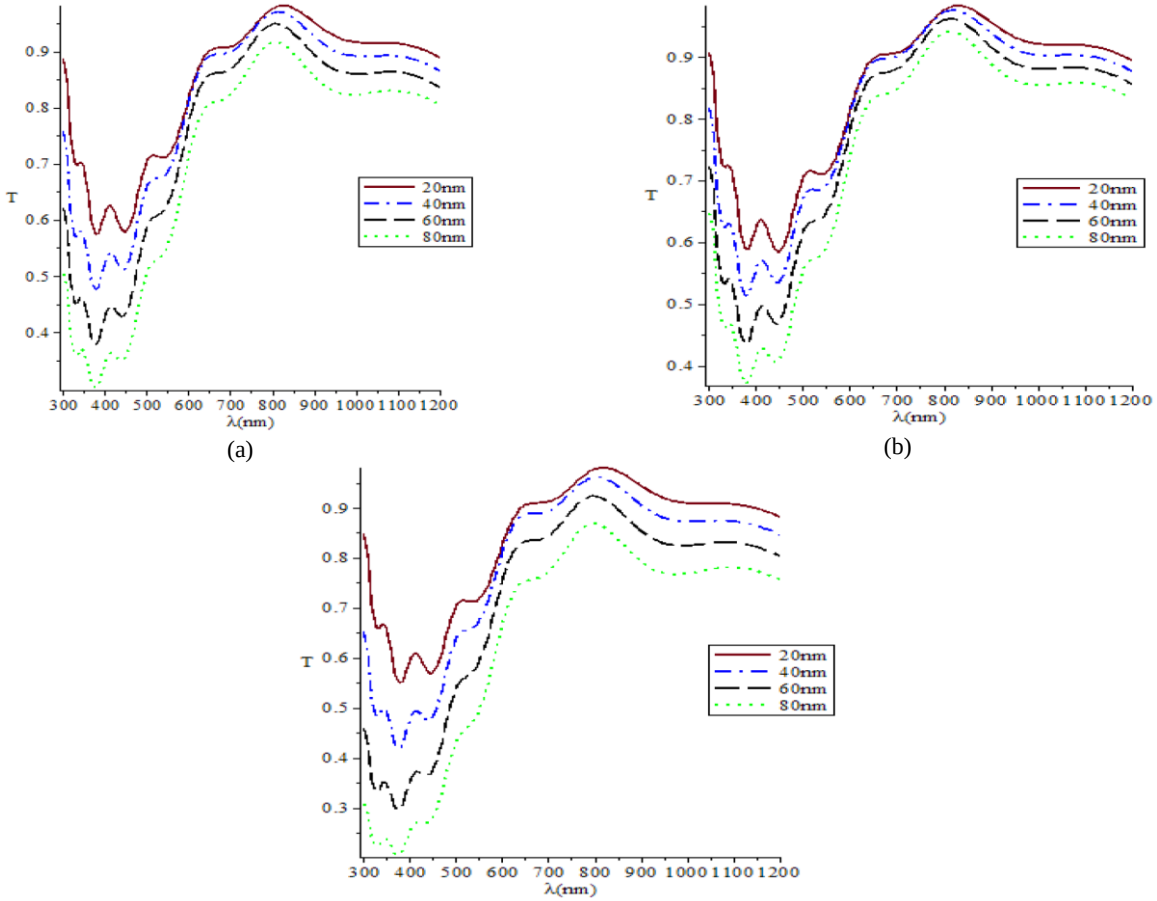

Fig. 6 – The transmitted light of the proposed structure for different active layer thicknesses doped by: a) Ag, b) Al, c) Au, and wavelength, and $CH_3NH_3PbBr_3$.

Figure 6 displays the transmitted light of the proposed structure for different active layer thicknesses doped by (Ag, Al, and Au), wavelength, and $CH_3NH_3PbBr_3$. It shows that transmission values in all wavelength ranges are better than those in the range of approximately 300–500 nm because of the perovskite reflectance in this range.

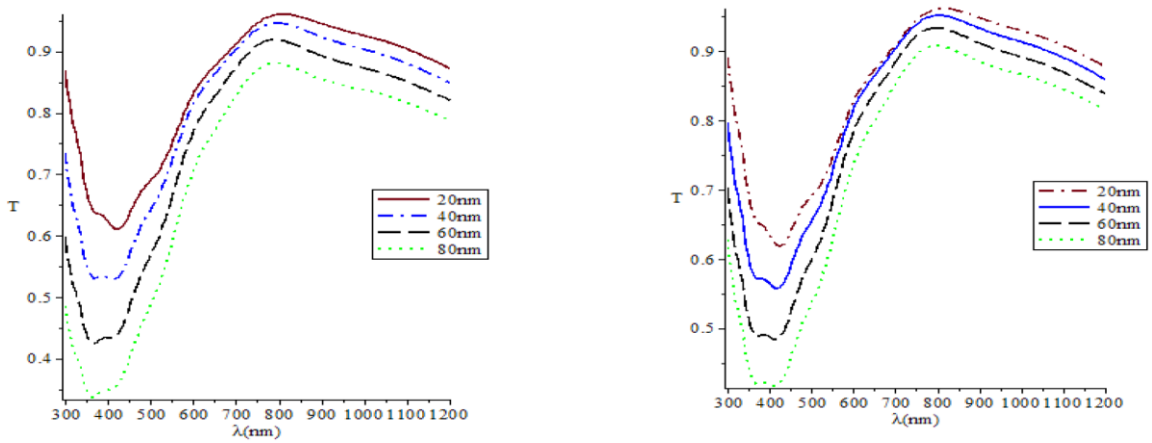

(a) (b)

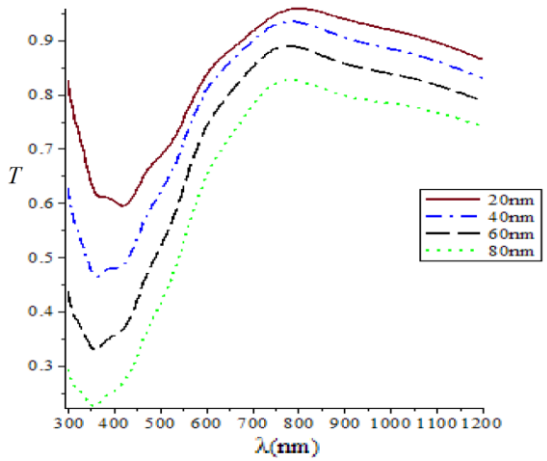

(c)

Fig. 7 – The transmitted light of the proposed structure for different active layer thicknesses doped by: a) Ag, b) Al, c) Au, and wavelength, and $CH_3NH_3PbI_2Br$.

Figure 7 plots the transmitted light of the proposed structure for different active layer thicknesses doped by (Ag, Al, and Au) and wavelength, and $CH_3NH_3PbI_2Br$, this cell shows similar values to the other cells with different perovskite types. The transmittance is decreasing due to the total destructive interference conditions that will gradually be achieved as the thickness of the perovskite increases.

Figures 5, 6, and 7 plot the transmitted light of the proposed structure for different $CH_3NH_3PbI_3$, $CH_3NH_3PbBr_3$, and $CH_3NH_3PbI_2Br$ perovskite types and glass layer doped by (Ag, Al, and Au) nanoparticles at $f = 0.25$ with different thicknesses 20, 40, 60, 80 nm and wavelength. 800 nm wavelength has the highest transmission values in $CH_3NH_3PbI_3$, $CH_3NH_3PbBr_3$ perovskite and, 750 nm at $CH_3NH_3PbI_2Br$ perovskite-type and it has a low reflection at different thicknesses and different nanoparticles type.

4. CONCLUSIONS

This paper proposed new perovskite and nanoparticle-based solar cells configurations. To establish the proposed cell's average transmission, the transfer matrix method was applied. We found that as the nanoparticles volume fraction increase, then, the transmission decrease, Cells doped with aluminum nanoparticles showed the best transmittances values compared with cells doped with silver and gold, and the minimum value for the transmission goes to the high wavelength from approximately 400 – 420 – 450 nm when we transmit $CH_3NH_3PbI_3$to $CH_3NH_3PbI_2Br$, $CH_3NH_3PbBr_3$. Also, when we describe the effect of active layer thickness on the transmittance we notice that after the range of wavelength over approximately 400 nm it increases approximately linearly until reaching its maximum value at about 800 nm, then it decreases.

REFERENCES

1. M.M. SHABAT, M.F. UBEID, *Antireflection coating at metamaterial waveguide structures for solar energy applications*, Energy Procedia, **50**, pp. 314–321, 2014.
2. H. MOUSA, *Antireflection coating at metamaterial waveguide structure by using superlattices (LANS)*, Journal of Modern Physics, **5**, *8*, art. 46401, 2014.
3. D. SONG, P. CUI, T. WANG, D. WEI, M. LI, F. CAO, X. YUE, P. FU, Y. LI, Y. HE, B. JIANG, *Managing carrier lifetime and doping property of lead halide perovskite by postannealing processes for highly efficient perovskite solar cells*, The Journal of Physical Chemistry C, **119**, *40*, pp. 22812–22819, 2015.
4. J.Y. WANG, C.S. HUANG, S.L. OU, Y.S. CHO, J.J. HUANG, *One-step preparation of TiO2 anti-reflection coating and cover layer by liquid phase deposition for monocrystalline Si PERC solar cell*, Solar Energy Materials and Solar Cells, **234**, art. 111433, 2022.
5. S. ABU LEBDA, *Theoretical analysis of metamaterial-multilayer waveguide structures for solar cells*, Master thesis, Islamic University, Physics Department, Gaza, Palestine, 2016.

6. Y. LIU, F. LANG, T. DITTRICH, A. STEIGERT, C.H. FISCHER, T. KÖHLER, P. PLATE, J. RAPPICH, M.C. LUX-STEINER, M. SCHMID, *Enhancement of photocurrent in an ultra-thin perovskite solar cell by Ag nanoparticles deposited at low temperature*, RSC Advances, **7**, *3*, pp. 1206–1214, 2017.
7. B. SINGH, M.M. SHABAT, D.M. SCHAADT, *Wide angle antireflection in metal nanoparticles embedded in a dielectric matrix for plasmonic solar cells*, Progress in Photovoltaics: Research and Applications, **28**, *7*, pp. 682–690, 2020.
8. M. GREEN, E. DUNLOP, J. HOHL-EBINGER, M. YOSHITA, N. KOPIDAKIS, X. HAO, *Solar cell efficiency tables (version 57)*, Progress in Photovoltaics: Research and Applications, **29**, *1*, pp. 3–15, 2021.
9. N.K. NOEL, S.D. STRANKS, A. ABATE, C. WEHRENFENNIG, S. GUARNERA, A.A. HAGHIGHIRAD, A. SADHANALA, G.E. EPERON, S.K. PATHAK, M.B. JOHNSTON, A. PETROZZA, *Lead-freeorganic-inorganic tin halide perovskites for photovoltaic applications*, Energy & Environmental Science, **7**, *9*, pp. 3061–3068, 2014.
10. A. BHALLA, R. GUO, R. ROY, *The perovskite structure – A review of its role in ceramic science and technology*, Materials Research Innovations, **4**, *1*, pp. 3–26, 2000.
11. K. ABUSHAAR, M.M. SHABAT, D.M. EL-AMASSI, D.M. SCHAADT, *Optimization design of solar cell based on silver nanoparticles*, Journal of Nanoelectronics and Optoelectronics, **14**, *9*, pp. 1237–1241, 2019.
12. M.M. SHABAT, S.A. NASSAR, H.G. ROSKOS, *Modeling plasmonic solar cells with noble metal nanoparticles using the finite difference time domain method*, Romanian Journal of Physics, **65**, art. 609, 2020.
13. Y.M. ADWAN, M.M. SHABAT, *Optical simulations of Graded Index Materials for solar cells model structure, TE case*, 2020 International Conference on Promising Electronic Technologies (ICPET), IEEE, 2020, pp. 99–102.
14. S. SAJID, A.M. ELSEMAN, J. JI, S. DOU, D. WEI, H. HUANG, P. CUI, W. XI, L. CHU, Y. LI, B. JIANG, *Computational study of ternary devices: stable, low-cost, and efficient planar perovskite solar cells*, Nano-micro Letters, **10**, art. 51, 2018.
15. E.D. PALIK, *Handbook of optical constants of solids*, Vol. 3, Academic Press, 1998.
16. M.M. SHABAT, D.M. EL-AMASSI, D.M. SCHAADT, *Design and analysis of multilayer waveguides containing nanoparticles for solar cells*, Solar Energy, **137**, pp. 409–412, 2016.

Received October 18, 2022